

# Dynamic evolution of vortex dipoles

(Evolución dinámica de dipolos vorticosos)

E. Salinas-Rodríguez<sup>1</sup>, M.G. Hernández<sup>2</sup>, A. Torres<sup>1</sup>, F. Valderrama<sup>3</sup> and F.J. Valdés-Parada<sup>1</sup>

<sup>1</sup>*Departamento de Ingeniería de Procesos e Hidráulica, Universidad Autónoma Metropolitana, Iztapalapa, México, D.F., México.*

<sup>2</sup>*División de Ciencias Básicas e Ingeniería, Universidad Autónoma Metropolitana, Azcapotzalco, México, D.F., México*

<sup>3</sup>*Departamento de Ingeniería Eléctrica Universidad Autónoma Metropolitana, Iztapalapa, México, D.F., México*

Recebido em 8/11/2010; Aceito em 16/6/2011; Publicado em 7/10/2011

Vortex dipoles are fundamental in fluid mechanics. They are found in geophysics, engineering and industry. The two necessary conditions to generate them are a plane flow and a generating force. In this work, an experimental design to generate vortex dipoles in stratified beds is presented. Vortex rings were generated under different volumetric flow conditions. Through visualization techniques, three stages were observed during the evolution of the rings: an exponential stage associated with the injection of the tracer, a parabolic stage and finally a dissipative stage. From the experimental results, the Reynolds and Péclet numbers were computed indicating laminar flows and diffusive flows, respectively.

**Keywords:** vortex dipoles, visualization techniques, Reynolds number, Péclet number, stratified bed.

Los dipolos vorticosos son fundamentales en mecánica de fluidos. Se encuentran en geofísica, ingeniería y la industria. Las dos condiciones necesarias para generarlos son un flujo plano y una fuerza generadora. En este trabajo se presenta un diseño experimental para generar dipolos vorticosos en lechos estratificados. Se generaron anillos vorticosos bajo diferentes condiciones de flujo volumétrico. Durante la evolución de los anillos se observaron tres etapas, mediante técnicas de visualización: una etapa exponencial asociada con la inyección del trazador, una etapa parabólica y finalmente una etapa disipativa. A partir de los resultados experimentales se calcularon los números de Reynolds y Péclet e indicaron flujos laminares y difusivos, respectivamente.

**Palabras-clave:** dipolos vorticosos, técnicas de visualización, número de Reynolds, número de Péclet, lecho estratificado.

## 1. Introduction

A vortex dipole is an axial flow with two vortices of equal strength but opposite sign travelling through a fluid. Due to the fluid's viscosity, the vorticity spreads over a larger area and therefore, the dipole decreases in strength, it slows down and spirals towards the centre of the domain. Inside the dipole, the fluid flows along the streamlines, around the extreme of vorticity; the maximum velocity, in the positive  $x$  direction, occurs at the dipole axis [1]. One half of the dipole has positive vorticity, whereas the other half has negative vorticity, therefore its total circulation is zero. Outside this circle there is no vorticity and the flow is potential. Vortex dipoles are very stable structures and decay only when their kinetic energy is almost completely dissipated by friction. Analytically, the dipole dynamics had been studied through the Navier-Stokes equation,

considering different initial conditions, since its solution depends strongly on them.

The vortex dipoles are fundamental elements in the dynamics of complex fluids and take place in natural systems. They have been observed in the oceans and in the atmosphere [2], in airfoils [3-5], in animals as jellyfish and squid for propulsion [6], in plants growth and in spore spread [7]. Therefore, their application includes diverse areas of physics and engineering as: meteorology, aerodynamics, biology, super-fluids and industrial turbulent flows [8-9]. Their motions are practically bidimensional due to the presence of stratified fluids, the rotation of the system, or by the combination of both factors. In order to generate them, two conditions are necessary: a plane flow and a generating force [10-12]. Therefore, understanding the vortex dipole generation and dynamics is of great interest in physics and engineering.

<sup>1</sup>E-mail: sabe@xanum.uam.mx.

In this work a vortex dipole is generated by a horizontal impulse into a stratified fluid. The vorticity is advected (transport due to the motion of the fluid the particle is suspended in) by the induced flow and diffuses (movement of particles along concentration gradients). The basic purpose of this work is to present a simple and economical experimental design to generate dipole rings. To this end the article is organized as follows. Section 2 is devoted to the experimental equipment design. In Section 3 we present the results of our experiments and in Section 4 we summarize our conclusions and discuss the scope and limitations of our work.

## 2. Experimental set-up and procedures

### 2.1. Experimental set-up and procedure

The experimental set-up consists of a container with its corresponding nozzle, and a measuring technique. Each component is explained in detail below.

### 2.2. Experimental container

The experiments were performed in a rectangular acrylic container  $0.3 \times 0.15 \times 0.06$  m and 0.012 m in wall thickness. A container with marble grain and a base of compacted rubber foam was used to avoid external disturbances during the experiments. Besides, the lamps container had an aired system to maintain constant the temperature of the fluids. The container was linearly stratified with common salt by diluting 80 g of salt per water liter. Distilled water was used as displacing fluid and food colorant (17 McCORMICK) was used as the displaced fluid. The fluids properties were measured at  $T = 24 \pm 0.5$  °C, the temperature,  $T$ , of the fluids and the interface were controlled by thermocouples type “J” of Constantan Iron (Kew Industries), through a digital analogical card of data acquisition (National Instruments) and Virtual software Bench-Logger. The shear viscosities of water and colorant were  $\mu_w = 0.0010019$  Pa.s and  $\mu_t = 0.01632$  Pa.s (Ostwald viscometer), respectively. Interfacial tension between water and colorant was  $\sigma = 58 \times 10^{-3}$  N/m (Fisher tensiometer). The densities were  $\rho_w = 997$  kg/m<sup>3</sup> for water and  $\rho_t = 1105.48$  kg/m<sup>3</sup> for the colorant (analytical balance, Ohaus). The container diameter was large enough so that wall effects can be assumed negligible. In Fig. 1 the schematic experimental apparatus is shown. The stratified bed was done with  $850 \times 10^{-6}$  m<sup>3</sup> of saline water and it was added in the container. The tracer liquid was injected to generate a horizontal jet flow from the nozzle. Later on, a vegetal sheet of paper was placed on it and  $275 \times 10^{-6}$  m<sup>3</sup> of distilled water was carefully poured the sheet until

slightly cover the nozzle; finally, the sheet was carefully removed [10].

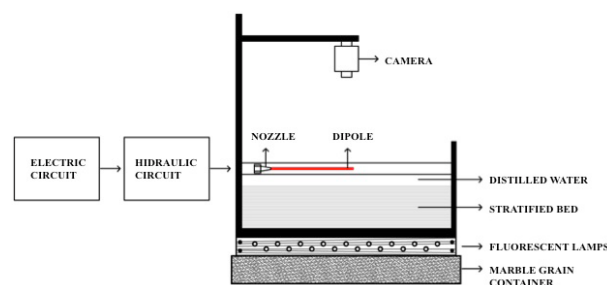


Figure 1 - Experimental set-up.

The tracer liquid was previously stored in a container and it was supplied with a regulated water pump (Jideco, model MC2-12) that generates a volumetric flow of  $(65.5 \pm 0.001) \times 10^{-6}$  m<sup>3</sup>/s, impelled with a motor of 12 V (CD) and a power of  $29 \times 10^{-3}$  Hp [13]. With a voltage source (Tektronix), the power necessary for the impelling motor of the pump was characterized resulting in the ability to control the volumetric flow with the opening of a control valve (Guss & Roch), obtaining volumetric flows from  $(3 \pm 0.001) \times 10^{-9}$  m<sup>3</sup>/s to  $(25 \pm 0.001) \times 10^{-9}$  m<sup>3</sup>/s through the nozzle. This automatized injection system controls the volumetric flow very precisely. It must be stressed that in Ref. [3] the tracer liquid was supplied by a burette manipulation. In Fig. 2, the hydraulic circuit is schematically shown.

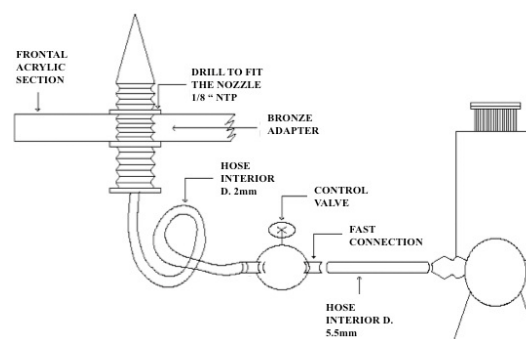


Figure 2 - Components of the hydraulic circuit.

Different volumetric flows,  $Q$ , were injected at the interface (stratified bed - distilled water) using a specially-designed bronze nozzle [14] with an inner diameter of  $d_n = 0.396 \times 10^{-3}$  m (Fig. 3). The tracer followed a straight line for a few seconds and subsequently it collapsed under gravity, forming a thin pancake-like region of horizontal motion that reorganizes into a dipolar structure. The dipole rings were generated in the stagnant liquid every 15 min, after changing the entire water system and allowing the liquid motion induced by this changes to be damped. This was done to avoid hydrodynamic interactions and changes in the density of the system by mixing. Besides the nozzle was cleaned every five experiments to avoid adhesions of the tracer

fluid on it, these adhesions could change the initial conditions of the system.

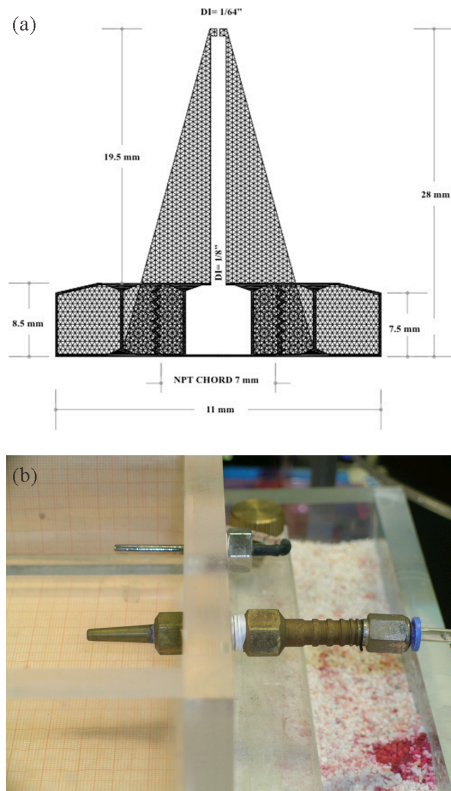


Figure 3 - Bronze nozzle (a) Schematic figure, (b) Photograph.

### 2.3. Technique of visualization and images treatment

The formation and evolution of the vortex ring was recorded with a video camera (Sony, CCDF50) at 30 frames per second. In order to avoid undesired reflections and shadows, as much as possible, a specific lightning array with four white light tubes was placed on a wood container; some orifices were made on it to avoid overheating. Also, a container with marble grain and a base of compacted rubber foam were placed below this array, to avoid external disturbances. The experiment took place in an entirely controlled environment. Ten experiments for three different volumetric flows:  $Q_0 = 10.4 \times 10^{-9} \text{ m}^3/\text{s}$ ,  $Q_1 = 11.0 \times 10^{-9} \text{ m}^3/\text{s}$  and  $Q_2 = 14.5 \times 10^{-9} \text{ m}^3/\text{s}$  were done. The images were digitized directly from the camera and later on, they were processed with AVI and DUB software. Finally individual frames were processed with the picture software Corel Draw 14, to obtain the data of each experiment.

### 3. Results and discussion

From the complete set of images, there were only considered those corresponding to each second. The first step in the analysis was to establish the beginning and end of the phenomena. The beginning of an experiment

was selected as the frame before the first displacement of the colorant. In addition, the end of an experiment was set up to correspond to the instant when the transverse displacement of the vortex ring reached a steady state. As a frame of reference, this instant was fixed to correspond to a distance of 4.5 cm from the nozzle in all cases. The second step was to calibrate the measurement of the longitudues. To this end the corresponding relation between the length measured from each image frame and the physical length were derived, by using the millimetric paper placed below the experimental container (Fig. 4).

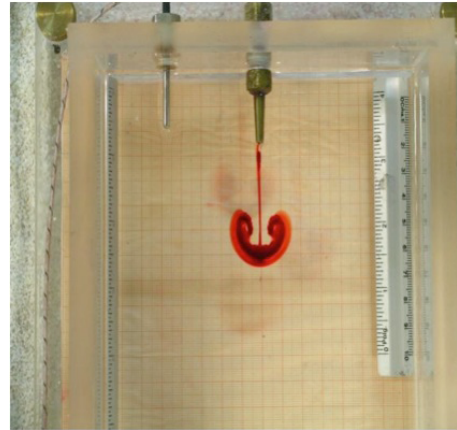


Figure 4 - Dipole ring.

Afterwards, the length and width of a vortex ring can be directly measured; as the rings were formed, the front of the transversal diameter of the ring was selected as the point for the measurements of transversal length. It is important to mention that the data treatment was made considering the trajectory along the center line, therefore if the dipole rings deviated from it, the uncertainty of the data increased.

An example of the measurements for  $Q_2$  is shown in Fig. 5. It must be stressed that the transverse displacement reaches the steady state before its longitudinal counterpart. Similar results were observed in the other experiments.

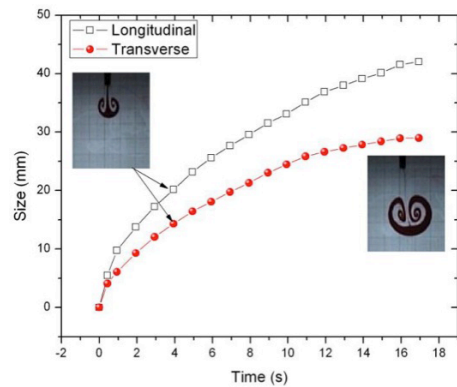


Figure 5 - Longitudinal and transverse displacements of the vortex ring vs. time for  $Q_1$ .

With these results the velocity can be computed

$$v_{i,j} = \frac{L_{i,j} - L_{i-1,j}}{t_i - t_{i-1}}, \quad j = L, T, \quad (1)$$

as well as the average velocity

$$\langle v \rangle_j = \frac{1}{N} \sum_{i=1}^{i=N} \frac{L_{i,j} - L_{i-1,j}}{t_i - t_{i-1}}, \quad j = L, T, \quad (2)$$

where  $N$  is the number of data.

An example of the evolution of the longitudinal  $\langle v \rangle_L$  and transverse  $\langle v \rangle_T$  components of the velocity is shown in Fig. 6. As expected, both velocities decrease with time, indicating a deceleration of the colorant spreading. The average velocities, computed using Eq. (2), were algebraically averaged to obtain the results shown

in Table 1. The uncertainty is one order of magnitude smaller than the computed velocity.

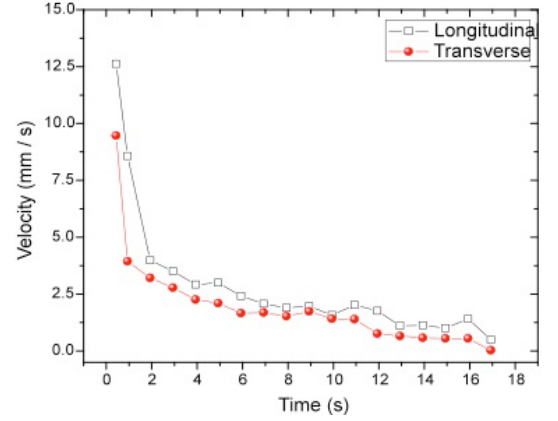


Figure 6 - Longitudinal and transverse velocity vs.  $t$  for  $Q_1$ .

Table 1 - Average longitudinal and transverse velocity for each flow rate.

Volumetric flow ( $\text{m}^3/\text{s}$ )	$\langle v \rangle_L$ (m/s)	$\langle v \rangle_T$ (m/s)	$\langle v \rangle_T / \langle v \rangle_L$
$Q_0$	$0.00177 \pm 0.0006$	$0.00113 \pm 0.0003$	$0.638 \pm 0.05$
$Q_1$	$0.00295 \pm 0.0000$	$0.00209 \pm 0.0001$	$0.708 \pm 0.03$
$Q_2$	$0.00304 \pm 0.0002$	$0.00215 \pm 0.0002$	$0.707 \pm 0.07$

From these results it can be appreciated that  $\langle v \rangle_T$  is always smaller than  $\langle v \rangle_L$ , it is consistent with the fact that viscosity spreads the vorticity over the area and thus slows down each monopole. Also, the rate  $\langle v \rangle_T / \langle v \rangle_L$  for  $Q_2$  is lower than  $Q_1$ , in contrast than we expect, nevertheless it is important to remember that the uncertainties for the velocities in the experiment 2 are bigger than in the experiment 1.

Since there is a concentration gradient, there is a diffusion process that obeys Ficks's law, and the diffusion coefficient  $D$  of the water-colorant system can be obtained in a crude estimation as

$$D = \frac{1}{N} \sum_{i=1}^{i=N} \frac{L_i L_{i-1}}{t_i - t_{i-1}}. \quad (3)$$

It is important to stress that  $D$  is an average quantity, in the sense that strictly, it should be defined as a statistical average over an ensemble with a number of molecules around the Avogadro number. In this work, we only considered two thousand frames to compute the axial diffusion and the results are given in Table 2. It can be observed that the uncertainty is one order of magnitude smaller than the computed diffusion coefficient. Nevertheless, the uncertainty for  $Q_0$  is greater than for  $Q_1$  and  $Q_2$ , the reason of it could be the deviation of the path from its center line. It must be stressed that this deviation could be produced by the external noise that are of the same order than the dynamic force

induced by  $Q_0$ .

Table 2 - Diffusion coefficient.

$Q$ ( $\text{m}^3/\text{s}$ )	$Q_0$	$Q_1$	$Q_2$
$D \times 10^5$ ( $\text{m}^2/\text{s}$ )	$1.27 \pm 1.3$	$1.70 \pm 0.316$	$1.96 \pm 0.5$

From Tables 1 and 2 it is evident that the best data belongs to the  $Q_1$ , and the uncertainty was lower than the other volumetric flows, for this stratified bed. Moreover, the best dipoles rings were developed for this flow; for the lowest,  $Q_0$ , the dipole rings deviated from the center line.

The Reynolds number  $Re = \rho_w \langle v \rangle d_n / \mu_w$  that establishes the relation between inertial and viscous forces, the Péclet number  $Pe \equiv \langle v \rangle d_n / D$  that gives the ratio between inertial and diffusive effects, and the Schmidt number that gives the ratio between viscous and diffusive effects,  $Sc \equiv \mu_w / (\rho_w D) = Pe / Re$ , were computed for the three volumetric flows. These numbers indicate the relative importance of two dynamical processes. The results are reported in Table 3.

Table 3 - Reynolds, Péclet and Schmidt numbers for different volumetric flows.

	$Re$	$Re$	$Pe$	$Sc$
$Q_0$	1.09	0.62	0.08	0.07
$Q_1$	1.33	0.92	0.07	0.05
$Q_2$	1.12	0.92	0.05	0.05

The longer each monopole remains close to the trajectory of the point vortex, the Reynolds is higher. For

dipoles vortex it is usually considered that the flow is laminar when the Reynolds number is lower than 100 [15]. As can be seen in Table 3, Reynolds number is between 0.693 and 1.497, therefore the flow regime is laminar. On the other hand, the Péclet number is between 0.079 and 0.115, so the inertial forces are 0.79% to 11.5% greater than diffusive forces. It can be seen that  $Pe_1 < Pe_2$ , but it is in the range of the experimental uncertainties values. The Schmidt number is between 0.053 and 0.166, indicating that the viscous effects are 5.3% to 16.6% greater than the diffusive effects. These values suggest that there is a diffusive flow, which might be due to the fact the tracer fluid's viscosity is sixteen times larger than that of water.

#### 4. Conclusions

In this work, a simple and economical experimental design to generate vortex rings in a stratified bed was presented, following the Afanasyev design [10], but introducing an automatized injection system and an antivibrational aired container. The former allows an accurate experiment's repeatability. The latter avoid the interaction between the external vibrations and the dipole dynamics.

The longitudinal and transversal longitudes were obtained with different visualization techniques and they were digitally analyzed. The software used is accessible at undergraduate and graduate courses. This experiment allows the students: to generate the vortex dipoles; to identify the parameters involved such as temperature, saline concentration, volumetric flow and the nozzle's internal diameter. The student also learns to analyze results with statistical methods.

The best vortex dipole corresponds to the largest volumetric flow. Nevertheless, the volumetric flow is of marginal importance in the dipoles average velocity for the saline concentration considered. Therefore, it is of importance to consider different saline concentrations in further work, as well as temperature gradients. Reynolds numbers showed laminar flows and the Péclet and Schmidt numbers showed diffusive flows.

The essential point to stress, though, is that this type of experiments allow the students to identify different flow regimes through the computed the obtained values of non-dimensional numbers as Reynolds, Péclet and Schmidt. Also, it is possible to observe how the qualitative behavior in this experiment is the analog to processes in nature and industries.

#### References

- [1] H.G.M. van Geffen, V.V. Meleshko and G.J.F. van Heijst, *J Physics of Fluids* **8**, 2393 (1996).
- [2] D.G. Dritschel and B. Legras, *Physics Today* **46**, 44 (1993).
- [3] M.D. Blokhina and Y.D. Afanasyev, *J Geophys Res Oceans* **108**, 3322 (2003).
- [4] <http://alex1.wordpress.com/fascinating-flows/>, accessed in July 1<sup>st</sup>, 2010.
- [5] J.H.B. Smith, *Ann Rev Fluid Mech* **18**, 221 (1986).
- [6] J.O. Dabiri, *Annu Rev Fluid Mech* **41**, 17 (2009).
- [7] D.L. Whitaker and J. Edwards, *Science* **329**, 406 (2010).
- [8] G.J.F. van Heijst, *Nederlands voor Tijdschrift Natuurkunde* **59**, 321 (1993).
- [9] R. Rajes and K. Mahesh, *J Flow Mechanics* **604**, 389 (2008).
- [10] Y. Afanasyev, *Am J Phys* **70**, 86 (2002).
- [11] D.J. Acheson, *Eur J Phys* **21**, 269 (2000).
- [12] O. Praud and A. Fincham, *J Flow Mech* **544**, 1 (2005).
- [13] C.L. Philips and D. Harbor, *Feedback Control of Systems, Design and Analysis of Electrical Processes and Controller* (Prentice Hall, Englewood Cliffs, 1996).
- [14] F. Valderrama, E. Salinas-Rodríguez, A. Torres and M.G. Hernández, *Prototype: Design, Automatization and Construction of a Container for Vortex Rings Generation* (Universidad Autónoma Metropolitana-Iztapalapa, Mexico City, 2009).
- [15] F. Rooij, P.F. Linden and S.B. Dalziel, *J Fluid Mech* **383**, 249 (1999).